Host infection by the grass-symbiotic fungus *Epichloë festucae* requires catalytically active H3K9 and H3K36 methyltransferases

Yonathan Lukito[1,2,3], Kate Lee[1], Nazanin Noorifar[1], Kimberly A. Green[1], David J. Winter[1], Arvina Ram[1], Tracy K. Hale[1], Tetsuya Chujo[1,4], Murray P. Cox[1], Linda J. Johnson[2], Barry Scott[1, 5]*.

[1]School of Fundamental Sciences, Massey University, Palmerston North 4442, New Zealand

[2]AgResearch Limited, Grasslands Research Centre, Palmerston North 4442, New Zealand

[5]Bio-Protection Research Centre, Massey University, Palmerston North 4442, New Zealand

*Corresponding author: School of Fundamental Sciences, Massey University, Palmerston North, New Zealand. Tel: (+64) 6 951 7705; Fax: (+64) 6 355 7953.

E-mail address: d.b.scott@massey.ac.nz (B. Scott).

[3]*Present Address: Ferrier Research Institute, Victoria University of Wellington, Wellington 6012, New Zealand*

[4]*Present Address: Research and Development Center, Mayekawa Mfg. Co., Ltd, Japan.*

Abstract

Recent studies have identified key genes in *Epichloë festucae* that control the symbiotic interaction of this filamentous fungus with its grass host. Here we report on the identification of specific fungal genes that determine its ability to infect and colonize the host. Deletion of *setB*, which encodes a homolog of the H3K36 histone methyltransferase Set2/KMT3, specifically reduced histone H3K36 trimethylation and led to severe defects in colony growth and hyphal development. The *E. festucae* Δ*clrD* mutant, which lacks the gene encoding the homolog of the H3K9 methyltransferase KMT1, displays similar developmental defects. Both mutants are completely defective in their ability to infect the host grass, and mutational studies of key residues in the catalytic SET domains from these proteins show that these phenotypes are dependent on the methyltransferase activities of SetB and ClrD. A comparison of the differences in the host transcriptome between seedlings inoculated with wild-type versus mutants suggests that the inability of these mutants to infect the host was not due to an aberrant host defense response. Co-inoculation of either Δ*setB* or Δ*clrD* with the wild-type strain enables these mutants to colonize the host. However, successful colonization by the mutants resulted in death or stunting of the host plant. Transcriptome analysis at the early infection stage identified four fungal candidate genes, three of which encode small-secreted proteins, that are differentially regulated in these mutants compared to wild-type. Deletion of *crbA*, which encodes a putative carbohydrate binding protein, resulted in significantly reduced host infection rates by *E. festucae*.

Author Summary

The filamentous fungus *Epichloë festucae* is an endophyte that forms highly regulated symbiotic interactions with the perennial ryegrass. Proper maintenance of such interactions is known to involve several signalling pathways, but much less is understood about the infection capability of this fungus in the host. In this study, we uncovered two epigenetic marks and their respective histone methyltransferases that are required for *E. festucae* to infect perennial ryegrass. Null mutants of the histone H3 lysine 9 and lysine 36 methyltransferases are completely defective in colonizing the host intercellular space, and these defects are dependent on the methyltransferase activities of these enzymes. Importantly, we observed no evidence for increased host defense response to these mutants that can account for their non-infection. Rather, these infection defects can be rescued by the wild-type strain in co-inoculation experiments, suggesting that failure of the mutants to infect is due to altered expression of genes encoding infection factors that are under the control of the above epigenetic marks that can be supplied by the wild-type strain. Among genes differentially expressed in the mutants at the early infection stage is a putative small-secreted protein with a carbohydrate binding function, which deletion in *E. festucae* severely reduced infection efficiency.

Introduction

Eukaryotic genomes are organised into discrete domains that are defined by the degree of chromatin condensation: euchromatin is generally less condensed and transcriptionally active, whereas heterochromatin is highly condensed and transcriptionally inactive [1]. The degree of chromatin condensation is controlled by various post-translational modifications of specific amino acid residues on the N-terminal tails of histones, including methylation, acetylation and phosphorylation [2, 3]. Cross-talk between the various protein complexes that modulate these histone modifications generates positive and negative feedback loops that control the final chromatin state and gene expression output [4, 5]. Among these various histone modifications, methylation of histone H3 is perhaps the most well-studied. Methylation of histone H3 lysine 4 (H3K4) and lysine 36 (H3K36) are associated with actively transcribed genes in euchromatic regions, whereas methylation of lysine 9 (H3K9) and lysine 27 (H3K27) is associated with the formation of constitutive and facultative heterochromatin, respectively [5]. These methyltransferase reactions are catalysed by SET domain proteins belonging to the COMPASS (K4), SET2 (K36), SpCLRC/NcDCDC (K9), and PRC2 (K27) protein complexes.

These histone marks and their respective methyltransferases are key regulators of fungal secondary metabolism [5-7], and are also required to establish and maintain the mutualistic interaction between the fungus *Epichloë festucae* and its grass host [8, 9]. Deletion of the *E. festucae* genes encoding the H3K9 methyltransferase ClrD or the H3K27 methyltransferase EzhB led to the derepression in culture of the subtelomeric *IDT* and *EAS* gene clusters, which encode the enzymes required for indole-diterpene (IDT) and ergot alkaloid (EAS) biosynthesis, respectively. Both mutations also impacted on the ability of *E. festucae* to form a symbiotic association with *L. perenne*; no host infection was observed after inoculation with the *clrD* mutant,

whereas plants infected with the *ezhB* mutant had a late onset host phenotype characterized by an increase in both tiller number and root biomass [8]. Deletion of the *cclA* gene, which encodes a homolog of the Bre2 component of the COMPASS (Set1) complex responsible for deposition of H3K4me3, also led to transcriptional activation of the *IDT* and *EAS* genes in axenic culture. In contrast, deletion of the *kdmB* gene, which encodes the H3K4me3 demethylase, decreased *in planta* expression of the *IDT* and *EAS* genes, and reduced levels of IDTs *in planta* [10]. Plants infected with the *cclA* or *kdmB* mutants have a host interaction phenotype that is similar to wild-type, demonstrating that loss of the ability to add (Δ*cclA*) or remove (Δ*kdmB*) H3K4me3 does not impact on the ability of *E. festucae* to establish a symbiosis. To complete our analysis of the four major histone H3 methyltransferases we examine here the role of *E. festucae* SetB (KMT3/Set2) in the symbiotic interaction.

Set2 was originally identified in yeast as an enzyme that induces transcriptional repression through methylation of histone H3K36 in yeast [11]. The Set2 protein interacts with the hyperphosphorylated form of RNA polymerase II (RNAPII) and catalyses methylation of H3K36 during transcriptional elongation [12-14]. A role for H3K36 methylation in transcriptional repression has been shown for both yeast and metazoans [11, 15-17]. More recent studies showed that presence of H3K36me3 in filamentous fungi is not associated with gene activation [18, 19], and has an important role in regulating fungal development and pathogenicity. Deletion of *SET2* homologs in *Magnaporthe oryzae* [20], *Fusarium verticillioides* [21], and *Fusarium fujikuroi* [19] led to growth defects in culture and reduced host pathogenicity. Culture growth defects were also observed for the corresponding mutants in *Neurospora crassa* and *Aspergillus nidulans* [22-25] highlighting the importance of Set2 for fungal development. Here we show that a catalytically

functional Set2 homolog is crucial for *E. festucae* to infect its host *L. perenne* and establish a mutualistic symbiotic association.

Results

SetB is an H3K36 methyltransferase that regulates fungal growth and development

The gene encoding the *E. festucae* homolog of the *Saccharomyces cerevisiae* H3K36 methyltransferase Set2 (KMT3) was identified by tBLASTn and named *setB* (gene model no. EfM3.042710; [26]). Protein structure analysis identified canonical PreSET, SET, PostSET, WW and SRI domains along with an additional TFS2N domain (Fig 1A), as reported for the *N. crassa* Set2 homolog [5]. *E. festucae setB* was deleted by targeted gene replacement using a *nptII* geneticin resistance cassette for selection. PCR screening of Gen^R transformants and Southern blot analysis identified a single Δ*setB* strain (S1 Fig). Western blot analysis of total histones showed that H3K36me3 was specifically depleted in this Δ*setB* strain, while levels of H3K36me1/2 were increased (Fig 1C). Introduction of the *setB* wild-type allele restored these methylation defects, confirming the role of SetB in H3K36 methylation (Fig 1C). This Δ*setB* strain grew extremely slowly in culture compared to the wild-type strain, a phenotype that was complemented by re-introduction of the *setB* wild-type allele (Fig 1D). Microscopic analysis of the hyphal morphology revealed that Δ*setB* hyphae had a wavy pattern of growth, branched more frequently and had hyphal compartments that were significantly shorter than observed for the wild-type strain (Fig 1E).

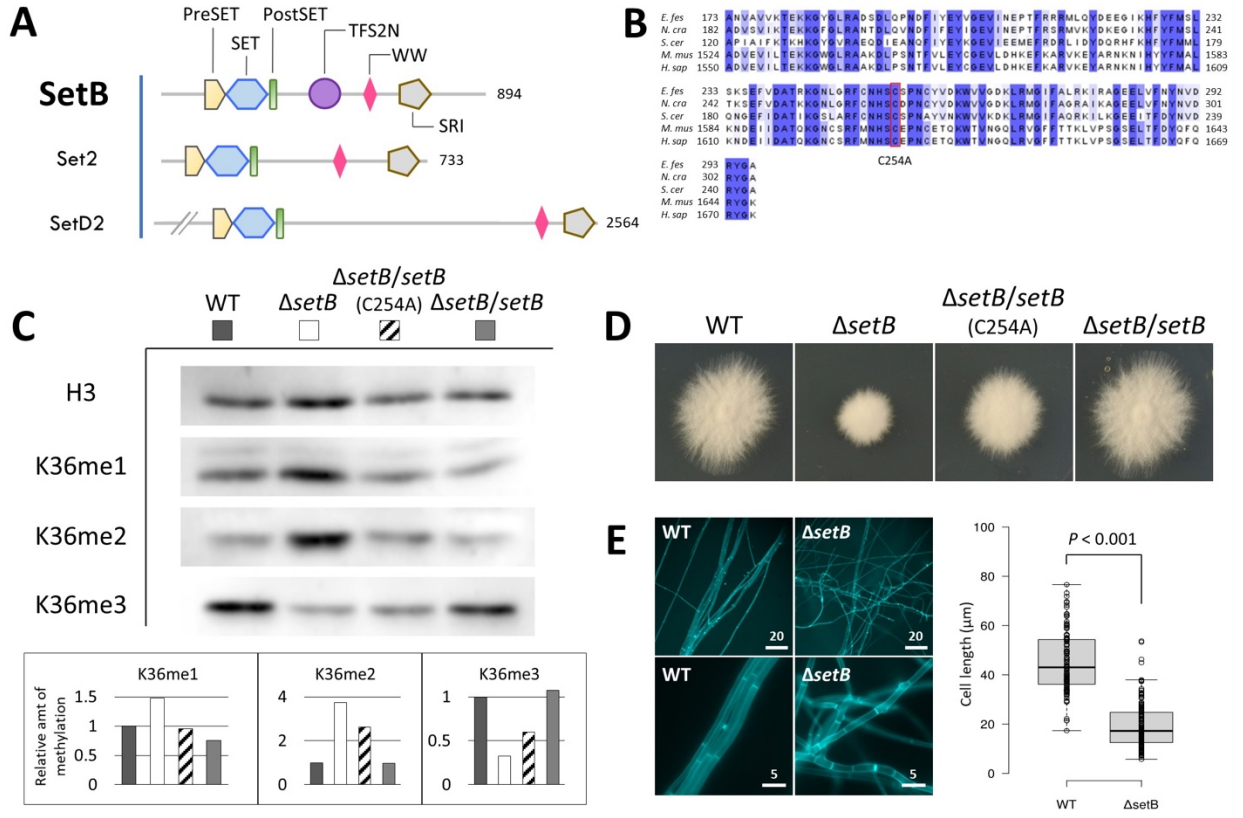

Fig 1. *E. festucae* SetB is an H3K36 methyltransferase. (A) Domain structure of *E. festucae* SetB and the yeast and mammalian orthologs. Numbers indicate the protein length in amino acids. (B) Amino acid alignment of SET domains of SetB and other SET2 proteins showing conservation of the cysteine 254 residue that was mutated to alanine in this study. (C) Western blot of total histones show reduced H3K36me3 and accumulation of H3K36me1/2 in Δ*setB*. Relative histone methylation was quantified by comparison to H3 band intensities, with the wild-type value arbitrarily set to 1. (D) Colony morphology after 6 days of growth in culture. (E) Deletion of *setB* affected hyphal morphology and length. Numbers above scale bars refer to length in µm. Boxplots represent more than 80 measurements of hyphal compartment lengths for each strain. The horizontal centre line of the boxes represent the medians and the top and bottom edges of the boxes represent the 75th and 25th percentiles, respectively.

The H3K36 methyltransferase activity of SetB is required for *E. festucae* to infect *Lolium perenne*

To study the role of SetB in the symbiotic interaction of *E. festucae* with its host, *L. perenne* seedlings were inoculated with Δ*setB* and grown for 8-12 weeks, after which time mature plant tillers were tested for infection by an immunoblot assay using an antibody raised against *E. festucae*. Four independent inoculation experiments revealed that Δ*setB* was unable to infect these host plants (Table 1, Fig 2A). The absence of the mutant in these mature plants was confirmed by confocal laser-scanning microscopy (CLSM) (Fig 2B). To determine if Δ*setB* failed to infect and colonize leaf tissue, or whether it was lost from the leaf tissue during tiller growth (reduction of endophyte persistence), we also examined the infection status of seedlings at one- and two-weeks post inoculation (wpi) by CLSM. At both timepoints, both endophytic and epiphytic hyphae of wild-type were observed at the infection site, but only epiphytic and not endophytic hyphae of Δ*setB* (Fig 2C and D). These observations demonstrate that Δ*setB* is completely unable to colonize the host at the site of infection. Re-introduction of the wild-type *setB* allele into the mutant restored the ability of this strain to infect *L. perenne* (Fig 2B, Table 1).

Subsequently, we sought to determine whether the phenotypes observed for Δ*setB* were caused by the lack of H3K36 trimethylation in this strain. Substitution of a conserved cysteine residue for alanine in the SET domain of *Neurospora crassa* SET-2 has previously been shown to result in a severe reduction in methyltransferase activity, confirming the importance of this amino acid for enzyme activity [11]. We therefore substituted alanine for the corresponding C254 residue in *E. festucae* SetB (Fig 1B) and tested if this allele was able to complement the H3K36 methylation, culture growth and host infection defects of Δ*setB*. Introduction of this $setB^{C254A}$ allele only partially rescued the H3K36me3 defect of Δ*setB*, as well as the aberrant accumulation of

159 H3K36me1/2 observed for this strain (Fig 1C). Likewise, the colony growth (Fig 1D) and host
160 infection phenotypes (Table 1) were only partially rescued by introduction of this allele. Although
161 the Δ*setB*/*setB*^{C254A} strain was able to infect the host, infection was at a significantly lower rate
162 than the Δ*setB*/*setB* complement or the wild-type strains (Table 1). Plants that were successfully
163 infected with the Δ*setB*/*setB*^{C254A} strain were phenotypically similar to wild-type infected plants
164 (S2 Fig). These results suggest that the phenotypes observed for Δ*setB* were due to the H3K36
165 methylation defects.

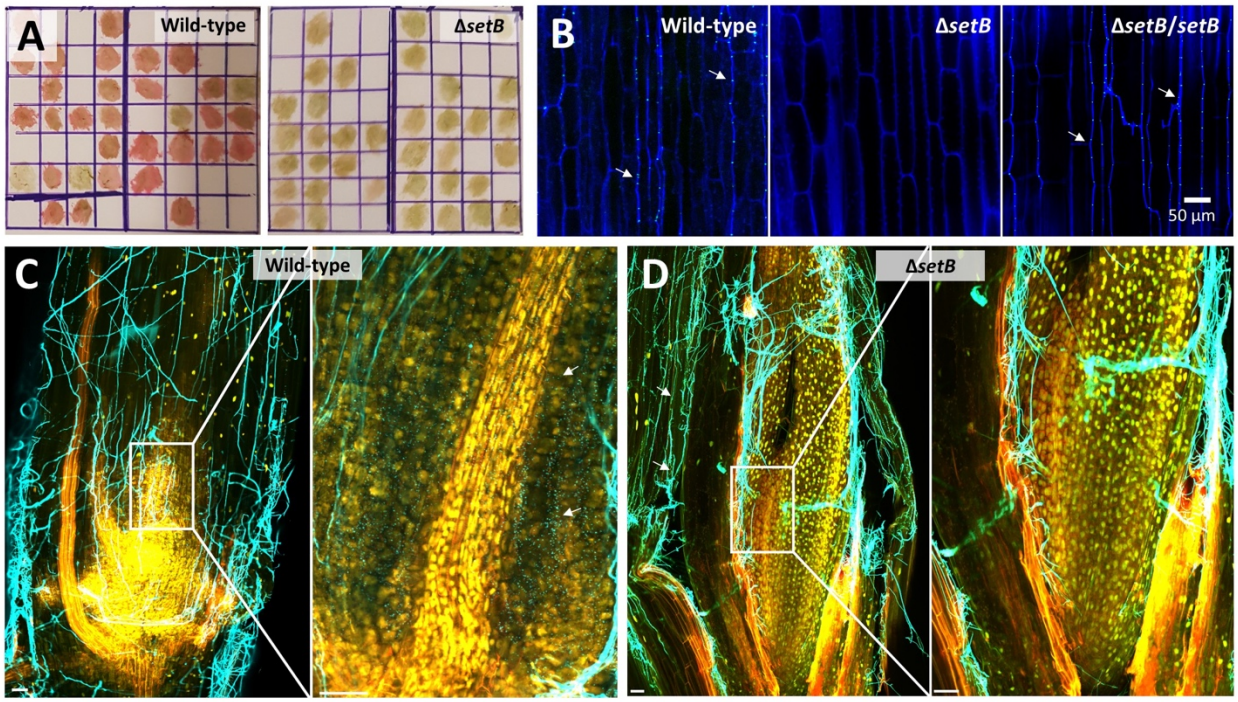

166

167 **Fig 2. *E. festucae setB* is required for host infection.** (A) Immunoblot detection of *E. festucae*
168 in plant tillers, visualized with Fast Red. (B) Confocal microscopy analysis of mature plant tillers.
169 Aniline blue was used to stain cell-wall glucans in hyphae (blue) and WGA-AF488 labels chitin
170 in fungal septa (cyan). Image of Δ*setB* showing absence of hyphae is representative of more than
171 10 plants analysed. z = 5 µm. (C & D) Confocal microscopy of 2 wpi seedlings stained with WGA-
172 AF488 (in cyan) indicate a presence of endophytic hyphae in seedlings infected with wild-type (C)

but not Δ*setB* (D). WGA-AF488 stains chitin in the cell wall of epiphytic hyphae but only stains the septa of endophytic hyphae. Images were generated by maximum intensity projection of z-stacks. Bars = 50 µm.

The H3K9 methyltransferase activity of ClrD is also required for host infection by *E. festucae*

The *E. festucae* Δ*clrD* mutant, which is defective in H3K9 mono-, di- and tri-methylation, also has a non-infection phenotype [8, 10]. However, that analysis did not differentiate lack of infection from lack of persistence as host plants were only examined for infection at 10-12 wpi. To discriminate between these two possibilities, we examined seedlings infected with mutant or wild-type at one- and two- wpi using CLSM. At both timepoints epiphytic and endophytic hyphae were observed for wild-type infected seedlings, but only epiphytic hyphae were observed at the inoculation site for Δ*clrD* (Fig 3). These observations suggest that Δ*clrD*, like Δ*setB*, is completely incapable of infecting the host plant. It is interesting to note that in addition to this non-infection phenotype, Δ*clrD* also shares several other phenotypes with Δ*setB*, including a slow growth rate on PDA (Fig 4A) and aberrant hyphal and cellular morphologies (Fig 4B).

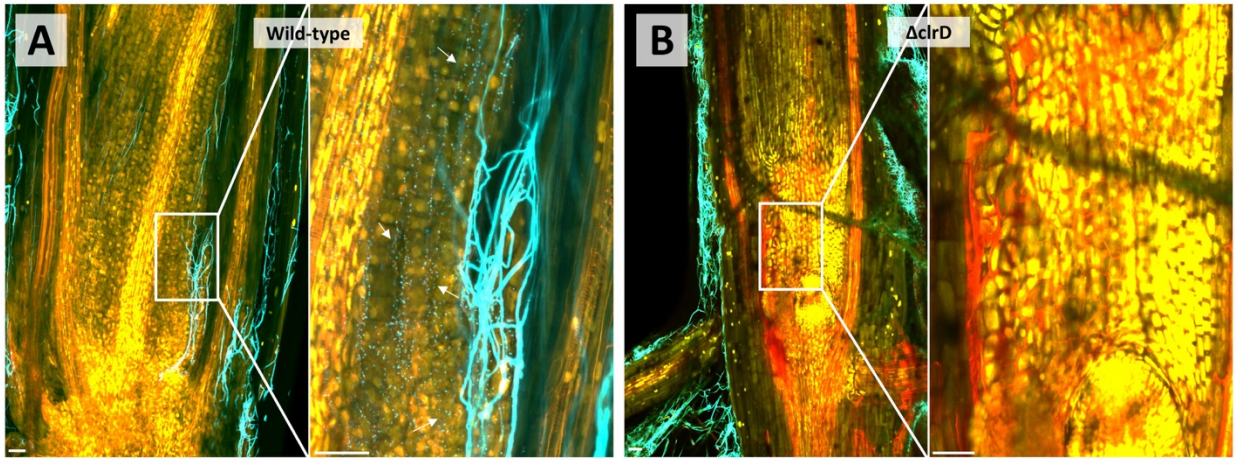

Fig 3. *E. festucae clrD* is required for host infection. Confocal microscopy of 2 wpi seedlings stained with WGA-AF488 (cyan) showing presence of epiphytic and endophytic hyphae in seedlings inoculated with wild-type (A) but only epiphytic hyphae for Δ*clrD* (B). Images were generated by maximum intensity projection of z-stacks. Bars = 50 µm.

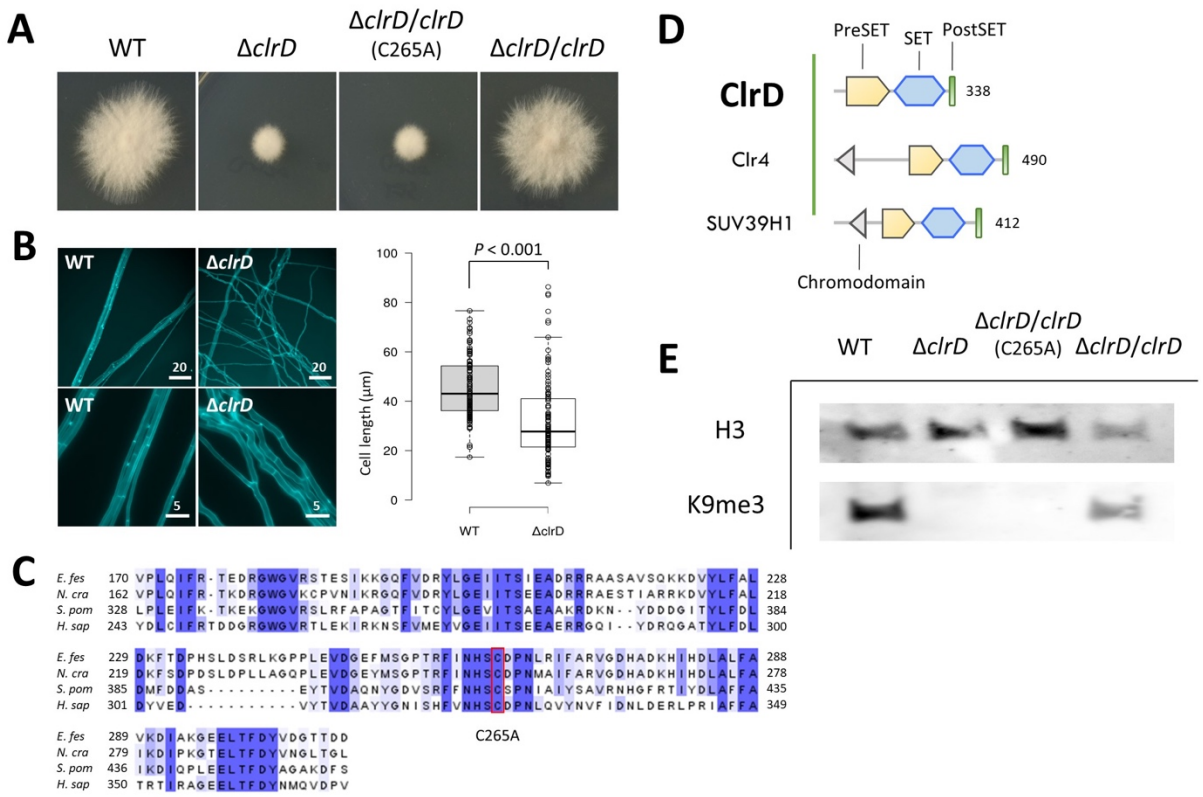

Fig 4. *E. festucae* ClrD is a H3K9 methyltransferase. (A) Colony morphology after 6 days of growth in culture. (B) Deletion of *clrD* affected hyphal morphology and length. Numbers above scale bars refer to length in µm. Boxplots represent more than 80 measurements of hyphal compartment lengths for each strain. The horizontal centre line of the boxes represent the medians and the top and bottom edges of the boxes represent the 75th and 25th percentiles, respectively. (C) Amino acid alignment of SET domains of ClrD and other KMT1 proteins showing conservation of the cysteine 265 residue that was mutated to alanine in this study. (D) Domain structure of *E. festucae* ClrD and the yeast and mammalian orthologs. Numbers indicate protein length in amino acids. (E) Western blot of total histones show reduced H3K9me3 in Δ*clrD*. Relative histone methylation was quantified by comparison to H3 band intensities, with the wild-type value arbitrarily set to 1.

To determine if the lack of H3K9 methyltransferase activity in the Δ*clrD* strain was responsible for the non-infection phenotype of the mutant [8], we tested if a *clrD*^{C265A} allele (Fig 4C & D) could complement the growth and H3K9 methylation defects of the Δ*clrD* mutant. The corresponding C265 residue in KMT1 (metazoan homolog of ClrD) is essential for the histone methyltransferase activity of the protein [27]. Likewise, we found that this allele failed to rescue the Δ*clrD* defects in H3K9 trimethylation (Fig 4E), colony growth (Fig 4A), and host infection (Table 1), indicating that the Δ*clrD* phenotypes observed were due to the absence of H3K9 methylation.

The infection-negative phenotypes of Δ*setB* and Δ*clrD* are not due to an altered host defense response

We next tested whether Δ*setB* and Δ*clrD* triggered an aberrant host defense response by measuring the expression of host defense genes in seedlings challenged with the mutants. *L. perenne* genes encoding proteins involved in the biotic stress response that were differentially expressed in response to infection with wild-type *E. festucae* Fl1 at seven wpi have previously been reported [28]. From this dataset we selected three of the most highly upregulated genes (m.131905, m.302781 and m.11574) and three of the most highly downregulated genes (m.41989, m.228647 and m.73716) with putative host defense functions (S3 Fig) and analysed their expression in seedlings at five days post inoculation (dpi) with wild-type, Δ*setB*, Δ*clrD*, or in mock-inoculated seedlings. None of these genes were significantly upregulated in plants inoculated with Δ*setB* or Δ*clrD* compared to wild-type (S3 Fig). One gene, m.11574 was significantly downregulated in the Δ*setB* compared to wild-type infected plants. This m.11574 gene was also the only differentially regulated gene in wild-type vs. mock-inoculated plants at five dpi, suggesting that expression of

these genes at this early time point is very different to expression in mature plants [28]. These results suggest that the mutants do not induce host defense responses more strongly than the wild-type strain. A host defense response can also present as a brown discoloration of the host tissues surrounding the inoculation site [29, 30]. However, no such browning of the host tissue was observed in seedlings inoculated with either Δ*setB* or Δ*clrD*.

Δ*clrD* and Δ*setB* are able to infect *L. perenne* if co-inoculated with the wild-type strain but give rise to incompatible associations

Finally we considered the possibility that Δ*clrD* and Δ*setB* do not produce permissive factors for infection, such as small secreted effector proteins. To this end, we tested if the wild-type strain, which would express such factors could rescue infection of the mutants. Seedlings were co-inoculated with mutant and wild-type mycelia at a 4:1 (mutant to wild-type) ratio to maximize the probability of the mutant entering the host. Infection was determined in mature plants (8 wpi) by immunoblot analysis and PCR was subsequently used to distinguish between wild-type and mutant endophyte strains present in these plants. Surprisingly, we were able to detect presence of the Δ*setB* mutant in 5/24 plants (S4A Fig), and the Δ*clrD* mutant in 1/13 plants (S4C Fig). The presence of PCR products for *setB* and *clrD* showed that the wild-type strain was also present in each of these plants (S4B and S4D Fig). This result indicates the wild-type strain facilitates host infection by the Δ*setB* and Δ*clrD* mutants.

To substantiate the above PCR results, we repeated the co-inoculation study using Δ*clrD* or Δ*setB* strains, constitutively expressing eGFP, together with wild-type expressing mCherry. We were able to observe both eGFP- and mCherry-expressing hyphae in the mature plant tissues by

CLSM, confirming that both Δ*clrD* and Δ*setB* mutants are able to infect if co-inoculated with the wild-type strain (Fig 5). In addition to individual eGFP- or mCherry-expressing hyphae, we also observed hyphae expressing both eGFP and mCherry (Fig 5A), the result of anastomosis between mutant and wild-type hyphae. A hyphal fusion test in axenic culture showed that the Δ*setB* and Δ*clrD* mutants were indeed capable of fusing with the wild-type strain (S5 Fig). However, the presence of individual eGFP-labelled hyphae in the plant indicates that this fusion with wild-type hyphae is not required for the mutants to enter the host, as it is not possible for anastomosed hyphae to re-segregate. Taken together, these results support the hypothesis that Δ*setB* and Δ*clrD* lack permissive factors for infection, which can be supplied by co-inoculation with the wild-type strain.

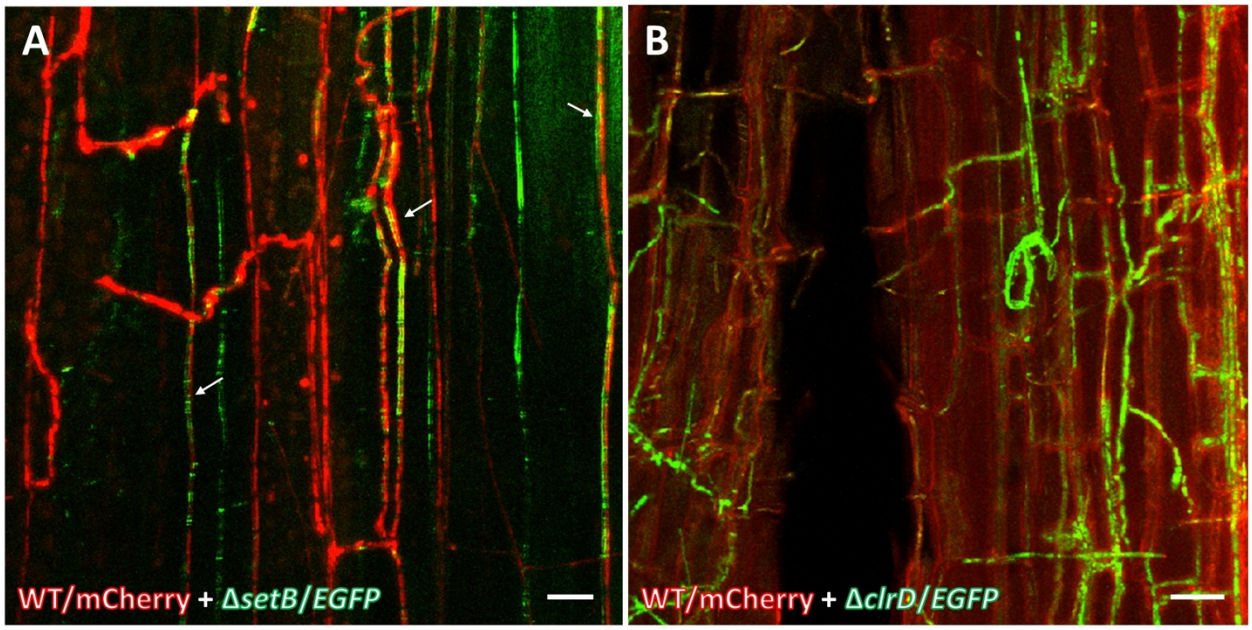

Fig 5. **Co-inoculation of Δ*setB* or Δ*clrD* with the wild-type strain enabled infection mutants to colonize the host.** (A) Confocal microscopy of plant tillers coinfected with mCherry-tagged wild-type and eGFP-tagged Δ*setB* strains. (B) Confocal microscopy of plant tillers coinfected with mCherry-tagged wild-type and eGFP-tagged Δ*clrD* strains. White arrows indicate hyphae expressing both mCherry and eGFP. Bars = 20 μm.

In addition to performing an immunoblot assay using anti-*E. festucae* antibody to determine infection in the co-inoculation experiment described above, we also performed a replica blot using anti-GFP antibody to determine the presence of the eGFP-labelled mutants in the infected plants. This revealed strong eGFP presence in a number of plants, all of which had underdeveloped root systems and just a single <10 cm tiller, and showed signs of senescence at 8 wpi (S6 Fig). Similar-aged ryegrass plants had >3 tillers and a height of >30 cm, indicating that presence of the Δ*setB* or Δ*clrD* mutants in the host may lead to host stunting. The remaining plants, which did not test positive for eGFP presence in the immunoblot, showed a range of host interaction phenotypes from severe stunting to normal growth (S7A and S7C Fig). To test the hypothesis that the stunted plants contained more mutant hyphae compared to the non-stunted plants, we isolated gDNA from these plants and performed qPCR analysis to measure the relative abundance of *eGFP* (marker) to *pacC* (control), a single-copy gene in *E. festucae* [31] In the Δ*setB*/*eGFP* co-inoculated plants, we detected the *eGFP* gene in four out of five stunted plants (80%), and in one of the six non-stunted plants (17%) (S7B Fig). In the Δ*clrD*/*eGFP* co-inoculated plants, we detected the *eGFP* gene in 11 out of the 14 stunted plants (79%), and in two of the seven non-stunted plants (29%) (S7D Fig). These results indicate that host stunting correlates with presence of the mutants inside the plants. Taken together, these results suggest that while Δ*setB* or Δ*clrD* hyphae are not able to infect the host on their own, when their infection is facilitated by co-inoculation with the wild-type strain, these mutants trigger a host response that results in stunting and premature death.

Transcriptomics of Δ*clrD* and Δ*setB* provide insights into *E. festucae* host infection process

To determine how the *E. festucae* and *L. perenne* transcriptomes are altered in the early stages of infection with wild-type or mutant strains, high throughput mRNA sequencing was performed on three biological replicates of *L. perenne* seedlings at three dpi with wild-type, Δ*clrD*, Δ*setB*, or a mock inoculation control. Fungal reads were mapped to the most recent *E. festucae* strain Fl1 gene model set [32], and the minimum definition for a differentially expressed gene (DEG) was defined as a statistically significant (S value ≤ 0.005) twofold change in gene expression between conditions (S1 File). This identified 1,027 DEGs in Δ*setB* vs. wild-type (746 downregulated and 281 upregulated), 705 DEGs in Δ*clrD* vs wild-type (333 down and 372 up), and a core set of 215 DEGs (160 down and 55 up) that were differentially regulated in both Δ*clrD* vs. wild-type and Δ*setB* vs. wild-type. Genes encoding predicted *E. festucae* effectors [33] are significantly over-represented in this core gene set (Fishers exact test, p=1 x 10^{-5}) comprising 5.6% (12/215) of this set compared to 1.2% (99/7,938) of all genes.

Four genes from these DEG sets stood out as candidate infection factors that might contribute to host colonization. These were identified by applying two criteria: first we looked for small secreted protein (SSP)-encoding genes that were upregulated in wild-type *in planta* at three dpi (this study) relative to axenic culture [9], which suggests they may play important roles during host infection (S2 File). Secondly, we searched for genes exhibiting strong differential expression in one or both of the Δ*clrD* and Δ*setB* mutants vs. wild-type. The first gene we identified, named *crbA* (EfM3.044610), encodes a putative 162 aa putative carbohydrate-binding protein, and is downregulated 114-fold to an almost silent state in Δ*setB*. The second gene (EfM3.066990), *dmlA* (domainless protein A), while not encoding an SSP, is entirely shut down in Δ*clrD* and encodes an 85 aa protein with no known domains. The third gene, *hybC* (EfM3.007740), encodes an 83 aa putative hydrophobin containing eight cysteine residues, a characteristic feature of hydrophobins

312 [34]. Expression of this gene is upregulated 600-fold at 3 dpi in wild-type vs. culture, and is
313 strongly downregulated in both Δ*setB* (250-fold) and Δ*clrD* (35-fold) vs. wild-type at 3 dpi. The
314 fourth gene, *sspZ* (EfM3.050840), encodes a putative 85 aa small secreted protein. This gene is
315 silent in wild-type axenic culture, minimally expressed at 3 dpi with wild-type, and upregulated in
316 Δ*setB* (7-fold) and Δ*clrD* (61-fold) at 3 dpi. Such upregulated genes are unlikely to encode proteins
317 required for infection but may represent genes that could impair *E. festucae* infection ability if
318 overexpressed. Three of these four genes, *crbA*, *hybC* and *sspZ*, were identified as candidate *E.*
319 *festucae* effectors [33, 35] (S1 file) and located in the sub-telomeric region of the Fl1 genome In
320 addition *crbA*, *dmlA* and *sspZ* genes are found proximal to AT-rich or repeat elements (S8 Fig),
321 which are regions of the *Epichloë* genome that are particularly enriched for symbiosis genes [32].
322 Two of these, *crbA* and *sspZ* are subtelomeric (S9 Fig). Interestingly, *crbA* appears to be a
323 component of a four-gene cluster present in some other *Epichloë* species (S1 Table, S10 Fig),
324 which is comprised of a divergently-transcribed gene encoding a chitinase (EfM3.044620),
325 together with genes encoding ankyrin domain protein (EfM3.104630) and a serine/threonine
326 kinase (EfM3.104640) (S10 Fig).

327 This 3 dpi transcriptome data also provided the opportunity to interrogate the host response
328 to *E. festucae* during the very early stages of the infection. Plant reads were mapped to our *L.*
329 *perenne* gene model set for which putative functions have been assigned [28], DEG minimum
330 requirements were set as above. Within the category of genes for "biotic" stress (n=830), 30 genes
331 were upregulated and one was downregulated in seedlings inoculated with wild-type compared to
332 mock (S3 File). By comparison, there were no upregulated genes within this category in seedlings
333 inoculated with Δ*setB* or Δ*clrD* compared to the wild-type strain (S4 File). Rather, five genes in
334 Δ*setB* and three in Δ*clrD*, were downregulated compared to the wild-type. The six genes analysed

in our RT-qPCR analysis (S4 Fig) were also not differentially expressed in this dataset. These results support the conclusion that Δ*setB* and Δ*clrD* do not induce an aberrant host defense response.

Functional analysis of genes encoding putative infection proteins

We next generated deletion strains of *hybC*, *crbA* and *dmlA* by targeted homologous recombination, as described above for *setB*, with 48 geneticin resistant transformants screened from each transformation using multiplex PCR. This analysis identified one transformant from each transformation in which the respective target gene was absent (S11A-C Fig). The targeted replacement of these genes was confirmed by PCR amplification across the left and right borders of deletion loci (S11A-C Fig), and multiplex PCRs were repeated with a high cycle number (45 cycles) to confirm absence of each gene in their corresponding mutant strain (S11D Fig). We also generated overexpression strains for *sspZ* by transforming wild-type with a construct placing *sspZ* under the control of the constitutively active P*tefA* promoter (S11E Fig). A total of 24 transformants were screened by qPCR and four transformants that contained the highest construct copy number in the genome, which ranged from 8-10 copies (S11E Fig), were selected for further analysis.

The culture colony morphology of all mutants was similar to the wild-type strain (S12 Fig). To test if the strains were disrupted in their ability to infect the host, they were inoculated into perennial ryegrass seedlings and the infection status of the plants was determined at nine wpi by immunoblotting. All mutants were observed to infect the host (S13 Fig); however, infection rates of the Δ*crbA* mutant, and to a lesser extent the Δ*dmlA* mutant, were significantly lower (S2 Table).

357 There were no differences in the gross morphology of mutant-infected plants from wild-type
358 infected plants at 10 wpi.

359

Discussion

The combination of both forward and reverse genetics studies in *Epichloë festucae* have identified key signaling pathways for the symbiotic interaction with the grass host, *Lolium perenne*. These include fungal cell wall integrity [36, 37], pheromone response/invasive growth [38], and stress-activated [39] mitogen-activated protein kinase (MAPK) pathways, cAMP [40], calcineurin [29], pH [31], light [41, 42], reactive oxygen species (ROS) [43-45] and lipid [46] signalling pathways. These genetic analyses uncovered host interaction phenotypes ranging from a mild alteration in the host tiller morphology to severe stunting of tiller growth. In the latter case, mutant hyphae exhibit pathogen-like proliferative growth within the host aerial tissues and colonize the host vascular bundles, phenotypes not observed for the wild-type [47]. *E. festucae* mutants defective in cell-cell fusion all exhibit this antagonistic host interaction phenotype, leading to the hypothesis that hyphal fusion and branching within the host plant are crucial for the establishment of a symbiotic hyphal network [47]. We have also identified a new class of symbiotic mutants defined by deletion of *clrD*, which encodes the histone H3K9 methyltransferase, that completely lack the ability to colonize the host [8]. In this study, we identified another mutant of this class, Δ*setB*, which lacks the histone H3K36 methyltransferase.

As shown by CLSM using aniline blue and WGA-AF488, both Δ*clrD* and Δ*setB* mutants are incapable of infecting and establishing an endophytic network of hyphae within the host, instead forming an epiphytic hyphal network around the site of inoculation. This inability to infect the host leaf cortical tissue is unlikely to be due to the slow growth rate phenotypes of the Δ*clrD* and Δ*setB* mutants because this is a phenotype also observed for the many infection-competent strains of *E. festucae* var *lolii* [48, 49]. *E. festucae* mutants of the small GTPases *racA* and *pakA* (*cla4*), which have similar slow growth phenotypes in culture, are also able to infect perennial

ryegrass [50, 51]. In fact, the vigorous epiphytic growth of Δ*clrD* and Δ*setB* and endophytic growth of Δ*racA* and Δ*pakA* suggest that growth in culture is not necessarily a reflection of the growth potential *in planta*.

Although the host and culture phenotypes of both mutants could be fully complemented by the wild-type alleles, the SET domain mutant allele $clrD^{C265A}$ failed to rescue both the host infection phenotype and the H3K9me3 defect. This result is consistent with the conserved cysteine residue being essential for the catalytic activity of KMT1 [27]. In contrast, the catalytic activity of SetB and the culture and infection phenotypes of the Δ*setB* mutant are only partially dependent on the conserved cysteine 254 residue of the SET domain of the protein. It is likely that the preceding arginine residue (R248), which is highly conserved and crucial for the activity of Set2 in *N. crassa* [11], is additionally required for the methyltransferase activity of SetB. The need for catalytically active ClrD and SetB highlights the important role H3K9 and H3K36 methylation have in regulating *E. festucae* host infection. Given the significance of these marks in transcriptional regulation, it is likely that misregulation of downstream genes are responsible for the infection defects of Δ*clrD* and Δ*setB*.

Surprisingly, co-inoculation with the wild-type strain enabled the mutants to infect and colonize the host plant. This suggests the wild-type strain is able to modulate the host environment to allow infection. However, co-infection resulted in host incompatibility, with host phenotypes varying from mild to severe stunting of the tillers, phenotypes observed previously for some other symbiotic mutants [47]. Severity of the host phenotype correlated with presence of mutant hyphae as determined by qPCR, a result consistent with phenotypes observed for a number of mutants that have a proliferative growth phenotype in the host [43, 45]. The presence of mutant hyphae in the host tissue was also confirmed by CLSM using strains expressing eGFP and mCherry. Importantly,

406 while CLSM showed that fusion between mutant and wild-type hyphae did occur, hyphae with
407 just one fluorescent marker were also present, highlighting that fusion with the wild-type hyphae
408 is not a prerequisite for host colonization by mutant hyphae after co-inoculation.

409 Since the completion of this study, another *E. festucae* mutant with a non-infection
410 phenotype, Δ*mpkB* has recently been isolated [38]. The *mpkB* gene is a homolog of the *N. crassa*
411 gene *mak-2*, which encodes the MAPK required for pheromone response/invasive growth
412 signaling [52]. As found for *N. crassa* Δ*mak-2* mutants, the *E. festucae* Δ*mpkB* mutant is also
413 defective in cell-cell fusion. The inability of Δ*mpkB* to infect the plant host is unusual as all other
414 *E. festucae* cell-cell fusion mutants isolated to date are still able to colonize host aerial tissues.
415 Given *mpkB* was not differentially expressed in either Δ*clrD* or Δ*setB* mutants at 3 dpi, it is
416 unlikely that the infection defects of these mutants are dependent on MpkB. Similarly, other genes
417 involved in the regulation of hyphal fusion in *E. festucae* are not differentially expressed in the
418 Δ*clrD* and Δ*setB* mutants at 3 dpi, including those of the ROS signaling pathway components
419 encoded by *noxA*, *noxR*, *racA* and *bemA* [43-45], or the cell wall integrity-MAPK pathway
420 components encoded by *mpkA*, *symB* and *symC* [36, 37]. All of these genes, including *mpkB*, are
421 essential for cell-cell fusion in *E. festucae* and for symbiosis with the host; however, the ability of
422 Δ*clrD* and Δ*setB* to anastomose indicates that these are a distinct class of mutants to both Δ*mpkB*
423 and the signaling pathways described above.

424 Major changes in the host transcriptome occur upon infection with *E. festucae*, suggesting
425 that the endophyte modulates host gene expression to establish a mutualistic symbiotic association
426 [28, 53, 54]. Among the host genes altered in the interaction between *E. festucae* strain Fl1 and *L.*
427 *perenne* are those involved in biotic stress response, including plant defense genes [28]. However,
428 none of these putative defense genes were aberrantly induced upon inoculation of *L. perenne*

seedlings with the Δ*clrD* or Δ*setB* strains at 3 dpi. RT-qPCR analysis for six of these putative defense genes that were previously shown to be differentially expressed at seven wpi [28] showed no statistically significant change in expression in host tissues from the infection site of seedlings at five dpi with the exception of one (m.11574), encoding a leucine-rich repeat receptor-like protein, which was instead downregulated in Δ*setB*-inoculated plants. This result was confirmed by a full transcriptome analysis of differences in host gene expression at three dpi where just five putative host defense genes were differentially expressed, all of which were downregulated in the Δ*clrD* or Δ*setB*-inoculated seedlings compared to seedlings inoculated with wild-type. In addition, the absence of any visual necrotic response as observed for ryegrass seedlings inoculated with a calcineurin mutant [29] suggests a hypersensitive response is not responsible for the lack of colonization by Δ*clrD* and Δ*setB*. Therefore, these mutants appear to be inherently incapable of infecting the host. In this respect, the ability of the wild-type strain to rescue infection in the co-inoculation experiments suggests that the wild-type strain secretes some factor into the extracellular environment which allows for host infection by these mutants.

Many plant-pathogenic fungi secrete small proteins that play important roles in pathogenicity and virulence. The tomato pathogen *Cladosporium fulvum* secretes LysM domain-containing effectors Avr4 and Ecp6 which function to bind and prevent host recognition of chitin, a major component of the fungal cell wall and a potent immunogen in plants [55, 56]. Other effectors directly modulate the host plant defense response, such as the *Ustilago maydis* effector Pit2 which inhibits host papain-like cysteine proteases central to the host apoplastic immunity [57, 58]. However, fungal effectors can also be important in mutualistic interactions as observed in the ectomycorrhizal fungus *Laccaria bicolor* which secretes an effector, MiSSP7, that regulates the symbiosis by modulating the host jasmonic acid signaling pathway [59, 60]. Modulation of the

host response by wild type secretion of effectors is one possible explanation for why co-inoculation of wild-type together with either Δ*clrD* or Δ*setB* enables these strains to infect the host. Candidate infection factors therefore include predicted small secreted proteins (SSPs) that are encoded by genes exhibiting both high expression by the wild-type *in planta*, and low expression by the Δ*clrD* and/or Δ*setB* mutants *in planta*. From the four predicted SSP genes selected for functional analysis, deletion of *crbA*, and to a lesser extent *dmlA*, led to significantly reduced infection rates. Deletion of *hybC* and overexpression of *sspZ*, which was upregulated in both Δ*clrD* and Δ*setB*, had no effect on the symbiotic interaction phenotype of *E. festucae*, possibly due to functional redundancy between SSPs [33, 61, 62]. These results show that while the ability to infect the host is a function of the cumulative effects of multiple gene products, some small secreted proteins can, and do, confer a significant individual contribution towards the efficiency of this process. Interestingly, *crbA* is also downregulated in the *E. festucae* Δ*hepA* mutant, which lacks the H3K9me3-binding Heterochromatin Protein I [9], as well as in three other symbiotic mutants Δ*sakA*, Δ*noxA* and Δ*proA* [63]. Intriguingly, *crbA* appears to be a component of a cluster of four genes encoding proteins important for cell wall (chitinase) and cell membrane (ankyrin) modifications. With the exception of *hybC* the three other genes analysed here are all found close to AT-rich or repeat-rich blocks of the genome, regions particularly enriched for fungal effectors [64, 65] and symbiotic genes [32].

Given the observation that chitin is masked or modified in endophytic but not epiphytic or axenic hyphae of *E. festucae* [66], remodelling of the fungal cell wall is also likely to be important for colonization and symbiosis. However, it is difficult to see how the wild-type strain could act *in trans* to complement this defect in the mutants. Instead, incomplete cell wall remodelling may explain the host incompatibility response elicited by Δ*clrD* and Δ*setB* once inside the plant. In

addition, while the Δ*crbA* and Δ*dmlA* mutants are compromised in their ability to infect, plants that are infected with these mutants do not reproduce the incompatibility phenotypes observed for plants co-infected with wild-type and Δ*clrD* or Δ*setB*. This is not surprising given that H3K9 and H3K36 methylation defects would affect the expression of a large number of genes, resulting in more dramatic phenotypes for these mutants. However, these host colonization and symbiosis defects appear to be specific to these two H3 marks as mutations that affect H3K4 and H3K27 methylation have little or no impact on the host interaction phenotype [8, 10].

H3K9 and H3K36 methylation play important roles in regulating fungal development and pathogenicity. Silencing of the *clrD* homolog, *DIM-5*, in *Leptosphaeria maculans* led to the aberrant overexpression of effector genes located near AT-isochores and attenuated pathogenicity in oilseed rape [67]. Deletion of the *clrD* and *setB* homologs, *Mokmt1* and *Mokmt3*, reduced the pathogenicity of *Magnaporthe oryzae* across several host plants [20]. Similarly, deletion of *set2* in *Fusarium verticillioides* led to reduced virulence and production of the mycotoxin bikaverin [21]. The growth defects of the Δ*clrD* and Δ*setB* mutants observed in this study are consistent with those observed in the *N. crassa* and *Aspergillus nidulans* mutants for these genes [22-25]. Interestingly, deletion of the *set2* homolog *ash1* in *Fusarium fujikuroi* led to a more severe developmental phenotype than deletion of *set2*, which is characterised by instability of subtelomeric chromosome regions and loss of accessory chromosomes, phenotypes associated with the proposed role of this paralog in DNA repair. Both mutants also had reduced host pathogenicity [19]. Given the global roles of ClrD and SetB in the maintenance of H3K9 and H3K36 methylation in the genome, it is likely that these proteins are not directly responsible for the infection ability of *E. festucae*, but rather this role is performed by other genes under their regulation.

498 In conclusion, we show here that ClrD-catalysed H3K9 and SetB-catalysed H3K36
499 methylation are crucial in regulating the ability of a fungal symbiont to infect its host. The results
500 of this study also underscore the importance of further analysis into the symbiotic roles and mode
501 of action of the small secreted protein encoded by the *crbA* gene, which appears to be important
502 for *E. festucae* infection efficiency.

503

504

Materials and methods

Fungal growth conditions, transformation and inoculation

Bacterial and fungal strains, plasmids, and plant material used in this study are listed in S3 Table. *E. festucae* strains were grown at 22°C on 2.4% (w/v) potato dextrose agar or broth with shaking at 200 rpm. *E. festucae* protoplasts were prepared and transformed as previously described [68, 69]. Inoculation of *E. festucae* perennial ryegrass seedlings was performed as previously described [70]. Plants were maintained in root trainers in an environmentally controlled growth room at 22°C with a photoperiod of 16 h of light (approximately 100 μE/m^2/s), and presence of endophyte was detected by immunoblot using anti-*E. festucae* antibody (AgResearch, Ltd), or anti-GFP antibody (Abcam ab290) as previously described [71]

Generation of DNA constructs and mutants

A list of PCR primers used in this study is provided in (S4 Table). Plasmid pYL23, which contains the *setB* replacement construct, was generated by Gibson assembly [72] from DNA fragments containing the 5' and 3' regions flanking *setB* that were amplified from an *E. festucae* Fl1 genomic DNA template using primer pairs YL286F/R and YL288F/R, respectively; a P*trpC*-*nptII*-T*trpC* gene expression cassette that confers geneticin resistance that was amplified from pSF17.1 using primers YL287F/R; and a *Nde*I-linearised pUC19 vector sequence. A linear fragment was excised from pYL23 by *Pac*I/*Spe*I digestion and used for transformation of wild-type *E. festucae* strain Fl1 protoplasts to generate Δ*setB* strains. A 4.3 kb DNA fragment covering the *setB* gene including promoter and terminator sequences was amplified from wild-type *E. festucae* genomic DNA using primers YL330F/R and ligated by blunt-end cloning into *Sna*BI-linearised pDB48 to generate the *setB* complementation plasmid pYL30. Plasmid pYL31,

527 containing the *setB*^{C254A} gene, was generated by site-directed mutagenesis of pYL30 using primer
528 pair YL378F/R. Plasmid pYL32, containing the *clrD*^{C265A} gene, was generated by site-directed
529 mutagenesis of pTC40 using primers YL379F/R. The sequence fidelity of all plasmid inserts were
530 confirmed by sequencing. For fluorescent tagging studies, Δ*setB* and Δ*clrD* protoplasts were
531 transformed with pCT74 harboring *eGFP* under the control of the *toxA* promoter.

532 Plasmid pYL41 containing the *hybC* replacement construct was generated by Gibson
533 assembly from DNA fragments amplified from an *E. festucae* Fl1 genomic DNA template using
534 primers YL459F/R (*hybC* 5' flank) and YL461aF/R (*hybC* 3' flank); the P*trpC*-*nptII*-T*trpC*
535 cassette amplified from pSF17.1 using primers YL460F/R, and *Nde*I-linearised pUC19. A linear
536 fragment for transformation was amplified from pYL41 by PCR using primers YL467F/R. The
537 *crbA* replacement construct-containing plasmid pYL43 was similarly generated from DNA
538 fragments amplified using primers YL464F/R (5' flank), YL466F/R (3' flank), YL465F/R (*nptII*
539 cassette), and *Nde*I-linearised pUC19. A linear fragment for transformation was amplified from
540 pYL43 by PCR using primers YL475F/R. The *dmlA* replacement construct-containing plasmid
541 pYL44 was similarly generated from DNA fragments amplified using primer YL486F/R (5' flank),
542 YL488F/R (3' flank), YL487F/R (*nptII* cassette), and *Nde*I-linearised pUC19. A linear fragment
543 for transformation was amplified from pYL44 by PCR using primers YL486F/488R. The *sspZ*
544 overexpression constructs pYL45 (with FLAG) and pYL46 (native) were generated by Gibson
545 assembly. For pYL45, the assembled DNA fragments included P*tef* amplified from pYL3 using
546 primers YL496F/R, *sspZ* amplified from wild-type *E. festucae* full-length cDNA using primers
547 YL497F/R, T*tub* amplified from pNR1 using primers YL498F/335R, and *Sna*BI-linearised
548 pDB48. For pYL46, the assembled DNA fragments included P*tef* amplified with primers
549 YL496F/496Rb from pYL3, *sspZ* was amplified from wild-type *E. festucae* full-length cDNA

using primers YL497Fb/497R, T*tub* amplified from pNR1 using primers YL498F/335R, and *Sna*BI-linearised pDB48.

For Southern blot analysis [73], DNA was digested and separated by electrophoresis, transferred to positively charged nylon membrane (Roche) and fixed by UV light cross-linking in a Cex-800 UV light cross-linker (Ultra-Lum) at 254 nm for 2 min. Labelling of DNA probes, hybridization, and visualization were performed using the DIG High Prime DNA Labeling & Detection Starter Kit I (Roche) as per the manufacturer's instructions.

RNA isolation, reverse transcription and quantitative PCR

Fungal and plant tissue were homogenized with mortar and pestle in liquid nitrogen and RNA was isolated using TRIzol (Invitrogen). For RT-qPCR analysis, cDNA was synthesized using the QuantiTect Reverse Transcription Kit (Qiagen) as per the manufacturer's instructions. qPCR was performed using the SsoFast™ EvaGreen Supermix (Bio-Rad) on a LightCycler® 480 System (Roche) according to the manufacturer's instructions with two technical replicates per sample. RT-qPCR was performed using absolute quantification and target transcript levels were normalized against the *E. festucae* reference genes *S22* (ribosomal protein S22; EfM3.016650) and *EF-2* (elongation factor 2; EfM3.021210) [8] or the *L. perenne* reference genes *POL1* (RNA polymerase I; m.40164) and *IMPA* (importin-a; m.15410) [28]. In all cases similar results were obtained by normalizing with either gene and only results normalized with *S22* or *POL1* are presented.

Histone extraction and western blotting

Histone extraction and western blot were performed as previously described [10]. In brief, fungal tissues were ground to a fine powder in liquid nitrogen, and nuclei were isolated by glycerol gradient centrifugation, sonicated, and histones were subsequently isolated by acid extraction.

572 **Microscopy and hyphal fusion**

573 Growth and morphology of hyphae *in planta* was determined by staining leaves with aniline blue
574 diammonium salt (Sigma) to stain fungal ß-1,3-glucans and Wheat Germ Agglutinin conjugated-
575 AlexaFluor488 (WGA-AF488; Molecular Probes/Invitrogen) to stain chitin, as previously
576 described [66]. While aniline blue itself is not fluorescent, there is a minor fluorochrome
577 component present, Sirofluor, that is fluorescent [74]. Hyphal growth and fungal cellular
578 phenotypes were documented by CLSM using a Leica SP5 DM6000B (Leica Microsystems)
579 confocal microscope outfitted with a 10×, NA 0.4, 40×, NA 1.3 or 63× NA 1.4 oil immersion
580 objective lens. WGA-AF488, to detect chitin, and aniline blue, to detect β-1,3-glucan, were excited
581 at 488 nm and 561 nm, respectively, and their emission spectra collected at 498-551 nm and 571-
582 632 nm respectively.

583 The culture eGFP-mRFP cell-cell fusion assays, were performed as previously described
584 [36]. For the coinfected mCherry-tagged wild-type and eGFP-tagged Δ*setB* strains and mCherry-
585 tagged wild-type and eGFP-tagged Δ*clrD* strains, unfixed pseudostem samples were examined by
586 CLSM (Leica SP5 DM6000B (Leica Microsystems)) using 488 nm and 561 nm DPSS laser.

587

588 **Bioinformatic analysis and transcriptomics**

589 The genome sequences of *E. festucae* were retrieved from the *E. festucae* Genome Project database
590 hosted by the University of Kentucky (http://csbio-l.csr.uky.edu/endophyte/cpindex.php) [26].
591 Protein domains were analysed with the SMART web-based tool (http://smart.embl-
592 heidelberg.de/) [75, 76]. Multiple amino acid sequence alignments were generated with Clustal
593 Omega (http://www.ebi.ac.uk/Tools/msa/clustalo/) [77, 78].

Scripts for the transcriptome and statistical analyses performed in this study are available from https://github.com/klee8/histone_mutants. Here we describe briefly each step of the analyses. The gene expression of Δ*setB* and Δ*clrD* was compared with wild-type by negative binomial regression for samples harvested three dpi. High-throughput mRNA sequencing was performed on three biological replicates for each of the wild-type, mock, Δ*setB* and Δ*clrD* associations. Samples were indexed and pooled before being sequenced across several Illumina NovaSeq 6000 lanes to reduce sample-to-sample technical variation. RNAseq read quality was assessed with FastQC v0.11.8 [79]. Adapter and poor-quality reads were removed with Trimmomatic v0.38 [80].

To find expression levels for each gene, read counts of each sample aligned against the *Epichloë* gene model set [32] were estimated with Salmon v0.13.1 [81]. The count data was imported into R v3.6.0 [82] using tximport v1.10.1 [83]. Genes that were significantly differentially expressed between mutant and wild type (s-value ≤ 0.005 and ≥ log 2-fold change) were identified with R package DESeq2 v1.22.2 [84] using the log2 fold shrinkage estimator implemented in apeglm v1.4.2 [85]. We accounted for multiple testing by using the s-value of Stephens [86].

A core set of highly up- and down-regulated genes for the Δ*setB* and Δ*clrD* mutants were identified using R. Genes were only included if their differential expression was in the same direction (i.e., all upregulated or all downregulated) in both mutants. Genes were annotated for putative signal peptides using SignalP v 5.0 [87, 88] and putative functions for encoded proteins were annotated using the online version of PANNZER2 [89]. The Δ*setB* and Δ*clrD* transcriptome data used here is available from the Sequence Read Archive (SRA) under BioProject PRJNA556310. A list of the individual biosample numbers is provided in S5 Table.

Similarly, the hypothesis that genes in Δ*setB* and Δ*clrD* mutants are differentially expressed *in planta* compared to axenic culture was tested by logistic regression, using previously published RNAseq data [9]. Analysis of *L. perenne* gene expression was carried out as for the *Epichloë* mutant gene expression analysis using the same quality-controlled RNAseq data, except that reads were aligned to the previously published *L. perenne* gene model set [28].

Acknowledgements

We thank Matthew Savoian (Manawatu Microscopy and Imaging Centre, Massey University) for technical advice and Daniel Berry and Berit Hassing (Massey University) for comments on this manuscript.

References

1. Grewal SI, Jia S. Heterochromatin revisited. Nat Rev Genet. 2007;8(1):35-46. Epub 2006/12/19. doi: nrg2008 [pii]

10.1038/nrg2008. PubMed PMID: 17173056.

2. Zhao Y, Garcia BA. Comprehensive catalog of currently documented histone modifications. Cold Spring Harbor perspectives in biology. 2015;7(9):a025064. Epub 2015/09/04. doi: 10.1101/cshperspect.a025064. PubMed PMID: 26330523; PubMed Central PMCID: PMCPMC4563710.

3. Zhou VW, Goren A, Bernstein BE. Charting histone modifications and the functional organization of mammalian genomes. Nat Rev Genet. 2011;12(1):7-18. Epub 2010/12/01. doi: 10.1038/nrg2905. PubMed PMID: 21116306.

4. Zhang T, Cooper S, Brockdorff N. The interplay of histone modifications - writers that read. EMBO Rep. 2015;16(11):1467-81. Epub 2015/10/18. doi: 10.15252/embr.201540945. PubMed PMID: 26474904; PubMed Central PMCID: PMCPMC4641500.

5. Freitag M. Histone methylation by SET domain proteins in fungi. Annu Rev Microbiol. 2017;71:413-39. doi: 10.1146/annurev-micro-102215-095757. PubMed PMID: 28715960.

6. Pfannenstiel BT, Keller NP. On top of biosynthetic gene clusters: How epigenetic machinery influences secondary metabolism in fungi. Biotechnology advances. 2019;37(6):107345. Epub 2019/02/10. doi: 10.1016/j.biotechadv.2019.02.001. PubMed PMID: 30738111; PubMed Central PMCID: PMCPMC6685777.

7. Brakhage AA. Regulation of fungal secondary metabolism. Nat Rev Microbiol. 2013;11(1):21-32. Epub 2012/11/28. doi: nrmicro2916 [pii]

652 10.1038/nrmicro2916. PubMed PMID: 23178386.

653 8. Chujo T, Scott B. Histone H3K9 and H3K27 methylation regulates fungal alkaloid
654 biosynthesis in a fungal endophyte-plant symbiosis. Mol Microbiol. 2014;92(2):413-34. Epub
655 2014/02/28. doi: 10.1111/mmi.12567. PubMed PMID: 24571357.

656 9. Chujo T, Lukito Y, Eaton CJ, Dupont PY, Johnson LJ, Winter D, et al. Complex
657 epigenetic regulation of alkaloid biosynthesis and host interaction by heterochromatin protein I
658 in a fungal endophyte-plant symbiosis. Fungal Genet Biol. 2019;125:71-83. Epub 2019/02/08.
659 doi: 10.1016/j.fgb.2019.02.001. PubMed PMID: 30731202.

660 10. Lukito Y, Chujo T, Hale TK, Mace W, Johnson LJ, Scott B. Regulation of subtelomeric
661 fungal secondary metabolite genes by H3K4me3 regulators CclA and KdmB. Mol Microbiol.
662 2019;112(3):837-53. Epub 2019/06/06. doi: 10.1111/mmi.14320. PubMed PMID: 31165508.

663 11. Strahl BD, Grant PA, Briggs SD, Sun ZW, Bone JR, Caldwell JA, et al. Set2 is a
664 nucleosomal histone H3-selective methyltransferase that mediates transcriptional repression. Mol
665 Cell Biol. 2002;22(5):1298-306. Epub 2002/02/13. doi: 10.1128/mcb.22.5.1298-1306.2002.
666 PubMed PMID: 11839797; PubMed Central PMCID: PMCPMC134702.

667 12. Li J, Moazed D, Gygi SP. Association of the histone methyltransferase Set2 with RNA
668 polymerase II plays a role in transcription elongation. J Biol Chem. 2002;277(51):49383-8. Epub
669 2002/10/17. doi: 10.1074/jbc.M209294200. PubMed PMID: 12381723.

670 13. Li B, Howe L, Anderson S, Yates JR, 3rd, Workman JL. The Set2 histone
671 methyltransferase functions through the phosphorylated carboxyl-terminal domain of RNA
672 polymerase II. J Biol Chem. 2003;278(11):8897-903. Epub 2003/01/04. doi:
673 10.1074/jbc.M212134200. PubMed PMID: 12511561.

674 14. Xiao T, Hall H, Kizer KO, Shibata Y, Hall MC, Borchers CH, et al. Phosphorylation of
675 RNA polymerase II CTD regulates H3 methylation in yeast. Genes Dev. 2003;17(5):654-63.
676 Epub 2003/03/12. doi: 10.1101/gad.1055503. PubMed PMID: 12629047; PubMed Central
677 PMCID: PMCPMC196010.
678 15. Landry J, Sutton A, Hesman T, Min J, Xu RM, Johnston M, et al. Set2-catalyzed
679 methylation of histone H3 represses basal expression of GAL4 in *Saccharomyces cerevisiae*.
680 Mol Cell Biol. 2003;23(17):5972-8. Epub 2003/08/15. doi: 10.1128/mcb.23.17.5972-5978.2003.
681 PubMed PMID: 12917322; PubMed Central PMCID: PMCPMC180946.
682 16. Furuhashi H, Takasaki T, Rechtsteiner A, Li T, Kimura H, Checchi PM, et al. Trans-
683 generational epigenetic regulation of *C. elegans* primordial germ cells. Epigenetics Chromatin.
684 2010;3(1):15. Epub 2010/08/14. doi: 10.1186/1756-8935-3-15. PubMed PMID: 20704745;
685 PubMed Central PMCID: PMCPMC3146070.
686 17. Rechtsteiner A, Ercan S, Takasaki T, Phippen TM, Egelhofer TA, Wang W, et al. The
687 histone H3K36 methyltransferase MES-4 acts epigenetically to transmit the memory of germline
688 gene expression to progeny. PLoS Genet. 2010;6(9):e1001091. Epub 2010/09/09. doi:
689 10.1371/journal.pgen.1001091. PubMed PMID: 20824077; PubMed Central PMCID:
690 PMCPMC2932692.
691 18. Connolly LR, Smith KM, Freitag M. The *Fusarium graminearum* histone H3 K27
692 methyltransferase KMT6 regulates development and expression of secondary metabolite gene
693 clusters. PLoS Genet. 2013;9(10):e1003916. Epub 2013/11/10. doi:
694 10.1371/journal.pgen.1003916
695 PGENETICS-D-13-01889 [pii]. PubMed PMID: 24204317.

19. Janevska S, Baumann L, Sieber CMK, Münsterkötter M, Ulrich J, Kämper J, et al. Elucidation of the two H3K36me3 histone methyltransferases Set2 and Ash1 in *Fusarium fujikuroi* unravels their different chromosomal targets and a major impact of Ash1 on genome stability. Genetics. 2018;208(1):153-71. doi: 10.1534/genetics.117.1119. PubMed PMID: 29146582; PubMed Central PMCID: PMC5753855.

20. Pham KT, Inoue Y, Vu BV, Nguyen HH, Nakayashiki T, Ikeda K, et al. MoSET1 (Histone H3K4 Methyltransferase in Magnaporthe oryzae) Regulates Global Gene Expression during Infection-Related Morphogenesis. PLoS Genet. 2015;11(7):e1005385. doi: 10.1371/journal.pgen.1005385. PubMed PMID: 26230995; PubMed Central PMCID: PMC4521839.

21. Gu Q, Wang Z, Sun X, Ji T, Huang H, Yang Y, et al. FvSet2 regulates fungal growth, pathogenicity, and secondary metabolism in *Fusarium verticillioides*. Fungal Genet Biol. 2017;107:24-30. Epub 2017/08/06. doi: 10.1016/j.fgb.2017.07.007. PubMed PMID: 28778753.

22. Tamaru H, Selker EU. A histone H3 methyltransferase controls DNA methylation in *Neurospora crassa*. Nature. 2001;414(6861):277-83. PubMed PMID: 11713521.

23. Adhvaryu KK, Morris SA, Strahl BD, Selker EU. Methylation of histone H3 lysine 36 is required for normal development in *Neurospora crassa*. Eukaryot Cell. 2005;4(8):1455-64. Epub 2005/08/10. doi: 10.1128/EC.4.8.1455-1464.2005. PubMed PMID: 16087750; PubMed Central PMCID: PMCPMC1214527.

24. Palmer JM, Perrin RM, Dagenais TR, Keller NP. H3K9 methylation regulates growth and development in Aspergillus fumigatus. Eukaryot Cell. 2008;7(12):2052-60. Epub 2008/10/14. doi: 10.1128/EC.00224-08. PubMed PMID: 18849468; PubMed Central PMCID: PMCPMC2593193.

719 25. Reyes-Dominguez Y, Bok JW, Berger H, Shwab EK, Basheer A, Gallmetzer A, et al.
720 Heterochromatic marks are associated with the repression of secondary metabolism clusters in
721 *Aspergillus nidulans*. Mol Microbiol. 2010;76:1376-86. Epub 2010/02/06. doi: MMI7051 [pii]
722 10.1111/j.1365-2958.2010.07051.x. PubMed PMID: 20132440.
723 26. Schardl CL, Young CA, Hesse U, Amyotte SG, Andreeva K, Calie PJ, et al. Plant-
724 symbiotic fungi as chemical engineers: multi-genome analysis of the Clavicipitaceae reveals
725 dynamics of alkaloid loci. PLoS Genetics. 2013;9(2):e1003323.
726 27. Rea S, Eisenhaber F, O'Carroll D, Strahl BD, Sun Z-W, Schmid M, et al. Regulation of
727 chromatin structure by site-specific histone H3 methyltransferases. Nature. 2000;406(6796):593-
728 9. PubMed PMID: 10949293.
729 28. Dupont PY, Eaton CJ, Wargent JJ, Fechtner S, Solomon P, Schmid J, et al. Fungal
730 endophyte infection of ryegrass reprograms host metabolism and alters development. New
731 Phytol. 2015;208(4):1227-40. doi: 10.1111/nph.13614. PubMed PMID: 26305687.
732 29. Mitic M, Berry D, Brasell E, Green K, Young CA, Saikia S, et al. Disruption of
733 calcineurin catalytic subunit (*cnaA*) in *Epichloë festucae* induces symbiotic defects and
734 intrahyphal hyphae formation. Mol Plant Path. 2018;19(6):1414-26. doi: 10.1111/mpp.12624.
735 PubMed PMID: 28990722.
736 30. Christensen MJ. Variation in the ability of *Acremonium* endophytes of *Lolium perenne*,
737 *Festuca arundinacea* and *F. pratensis* to form compatible associations in the three grasses.
738 Mycol Res. 1995;99(4):466-70.
739 31. Lukito Y, Chujo T, Scott B. Molecular and cellular analysis of the pH response
740 transcription factor PacC in the fungal symbiont *Epichloë festucae*. Fungal Genet Biol.
741 2015;85:25-37. doi: 10.1016/j.fgb.2015.10.008. PubMed PMID: 26529380.

742 32. Winter DJ, Ganley ARD, Young CA, Liachko I, Schardl CL, Dupont PY, et al. Repeat
743 elements organise 3D genome structure and mediate transcription in the filamentous fungus
744 *Epichloë festucae*. PLoS Genetics. 2018;14(10):e1007467. Epub 2018/10/26. doi:
745 10.1371/journal.pgen.1007467. PubMed PMID: 30356280.
746 33. Hassing B, Winter D, Becker Y, Mesarich CH, Eaton CJ, Scott B. Analysis of *Epichloë*
747 *festucae* small secreted proteins in the interaction with *Lolium perenne*. PLoS One.
748 2019;14(2):e0209463. Epub 2019/02/14. doi: 10.1371/journal.pone.0209463. PubMed PMID:
749 30759164; PubMed Central PMCID: PMCPMC6374014.
750 34. Wessels JGH. Fungal hydrophobins: proteins that function at an interface. Trends Plant
751 Sci. 1996;1:9-15.
752 35. Sperschneider J, Gardiner DM, Dodds PN, Tini F, Covarelli L, Singh KB, et al.
753 EffectorP: predicting fungal effector proteins from secretomes using machine learning. New
754 Phytol. 2016;210(2):743-61. doi: 10.1111/nph.13794. PubMed PMID: 26680733.
755 36. Becker Y, Eaton CJ, Brasell E, May KJ, Becker M, Hassing B, et al. The fungal cell wall
756 integrity MAPK cascade is crucial for hyphal network formation and maintenance of restrictive
757 growth of *Epichloë festucae* in symbiosis with *Lolium perenne*. Mol Plant-Microbe Interact.
758 2015;28:69-85. doi: doi:10.1094/MPMI-06-14-0183-R.
759 37. Green KA, Becker Y, Tanaka A, Takemoto D, Fitzsimons HL, Seiler S, et al. SymB and
760 SymC, two membrane associated proteins, are required for *Epichloë festucae* hyphal cell-cell
761 fusion and maintenance of a mutualistic interaction with *Lolium perenne*. Mol Microbiol.
762 2017;103:657-77. doi: 10.1111/mmi.13580. PubMed PMID: 27882646.
763 38. Tanaka A, Kamiya S, Ozaki Y, Kameoka S, Kayano Y, Sanjay S, et al. A nuclear protein
764 NsiA from *Epichloë festucae* interacts with a MAP kinase MpkB and regulates the expression of

765 genes required for symbiotic infection and hyphal cell fusion. Mol Microbiol. 2020. Epub
766 2020/07/08. doi: 10.1111/mmi.14568. PubMed PMID: 32634260.
767 39. Eaton CJ, Cox MP, Ambrose B, Becker M, Hesse U, Schardl CL, et al. Disruption of
768 signaling in a fungal-grass symbiosis leads to pathogenesis. Plant Physiol. 2010;153(4):1780-94.
769 Epub 2010/06/04. doi: pp.110.158451 [pii]
770 10.1104/pp.110.158451. PubMed PMID: 20519633.
771 40. Voisey CR, Christensen MT, Johnson LJ, Forester NT, Gagic M, Bryan GT, et al. cAMP
772 signaling regulates synchronised growth of symbiotic *Epichloë* fungi with the host grass *Lolium*
773 *perenne*. Front Plant Science. 2016;7:1546. doi: 10.3389/fpls.2016.01546. PubMed PMID:
774 27833620; PubMed Central PMCID: PMC5082231.
775 41. Rahnama M, Johnson RD, Voisey CR, Simpson WR, Fleetwood DJ. The global
776 regulatory protein VelA is required for symbiosis between the endophytic fungus *Epichloë*
777 *festucae* and *Lolium perenne*. Mol Plant Microbe Interact. 2018;31(6):591-604. Epub
778 2018/01/10. doi: 10.1094/MPMI-11-17-0286-R. PubMed PMID: 29315021.
779 42. Rahnama M, Maclean P, Fleetwood DJ, Johnson RD. The LaeA orthologue in *Epichloë*
780 *festucae* is required for symbiotic interaction with *Lolium perenne*. Fungal Genet Biol.
781 2019;129:74-85. Epub 2019/05/10. doi: 10.1016/j.fgb.2019.05.001. PubMed PMID: 31071427.
782 43. Takemoto D, Tanaka A, Scott B. A p67(Phox)-like regulator is recruited to control
783 hyphal branching in a fungal-grass mutualistic symbiosis. Plant Cell. 2006;18(10):2807-21.
784 PubMed PMID: 17041146.
785 44. Takemoto D, Kamakura S, Saikia S, Becker Y, Wrenn R, Tanaka A, et al. Polarity
786 proteins Bem1 and Cdc24 are components of the filamentous fungal NADPH oxidase complex.
787 Proc Natl Acad Sci USA. 2011;108(7):2861-6.

788 45. Tanaka A, Christensen MJ, Takemoto D, Park P, Scott B. Reactive oxygen species play a
789 role in regulating a fungus-perennial ryegrass mutualistic association. Plant Cell. 2006;18:1052-
790 66.
791 46. Hassing B, Eaton CJ, Winter D, Green KA, Brandt U, Savoian MS, et al. Phosphatidic
792 acid produced by phospholipase D is required for hyphal cell-cell fusion and fungal-plant
793 symbiosis. Mol Microbiol. 2020;113(6):1101-21. Epub 2020/02/06. doi: 10.1111/mmi.14480.
794 PubMed PMID: 32022309.
795 47. Scott B, Green K, Berry D. The fine balance between mutualism and antagonism in the
796 *Epichloë festucae*-grass symbiotic interaction. Curr Opin Plant Biol. 2018;44:32-8. doi:
797 10.1016/j.pbi.2018.01.010. PubMed PMID: 29454183.
798 48. Johnson LJ, De Bonth ACM, Briggs LR, Caradus JR, Finch SC, Fleetwood DJ, et al. The
799 exploitation of epichloae endophytes for agricultural benefit. Fungal Diversity. 2013;60(1):171-
800 88.
801 49. Christensen MJ, Bennett RJ, Schmid J. Growth of *Epichloë*/*Neotyphodium* and p-
802 endophytes in leaves of *Lolium* and *Festuca* grasses. Mycol Res. 2002;106:93-106.
803 50. Tanaka A, Takemoto D, Hyon GS, Park P, Scott B. NoxA activation by the small GTPase
804 RacA is required to maintain a mutualistic symbiotic association between *Epichloë festucae* and
805 perennial ryegrass. Mol Microbiol. 2008;68(5):1165-78. PubMed PMID: 18399936.
806 51. Becker Y, Eaton C, Jourdain I, Scott B. The role of *Epichloë festucae* RacA interacting
807 proteins, PakA, PakB, RhoGDI, on cell polarity in culture and synchronized growth in *Lolium*
808 *perenne*. 27th Fungal Genetics Conference; Asilomar, Pacific Grove, CA2013. p. Fungal
809 Genetics Reports 60 (Suppl): Abstract #612.

52. Pandey A, Roca MG, Read ND, Glass NL. Role of a mitogen-activated protein kinase pathway during conidial germination and hyphal fusion in *Neurospora crassa*. Eukaryot Cell. 2004;3(2):348-58. Epub 2004/04/13. PubMed PMID: 15075265; PubMed Central PMCID: PMC387641.

53. Schmid J, Day R, Zhang N, Dupont PY, Cox MP, Schardl CL, et al. Host tissue environment directs activities of an *Epichloë* endophyte, while it induces systemic hormone and defense responses in its native perennial ryegrass host. Mol Plant-Microbe Interact. 2016;30(2):138-49. doi: 10.1094/MPMI-10-16-0215-R. PubMed PMID: 28027026.

54. Ambrose KV, Belanger FC. SOLiD-SAGE of endophyte-infected red fescue reveals numerous effects on host transcriptome and an abundance of highly expressed fungal secreted proteins. PLoS One. 2012;7(12):e53214. doi: 10.1371/journal.pone.0053214. PubMed PMID: 23285269; PubMed Central PMCID: PMC3532157.

55. de Jonge R, van Esse HP, Kombrink A, Shinya T, Desaki Y, Bours R, et al. Conserved fungal LysM effector Ecp6 prevents chitin-triggered immunity in plants. Science. 2010;329(5994):953-35. Epub 2010/08/21. doi: 329/5994/953 [pii]

10.1126/science.1190859. PubMed PMID: 20724636.

56. van den Burg HA, Harrison SJ, Joosten MH, Vervoort J, de Wit PJ. *Cladosporium fulvum* Avr4 protects fungal cell walls against hydrolysis by plant chitinases accumulating during infection. Mol Plant-Microbe Interact. 2006;19(12):1420-30. PubMed PMID: 17153926.

57. Mueller AN, Ziemann S, Treitschke S, Assmann D, Doehlemann G. Compatibility in the *Ustilago maydis*-maize interaction requires inhibition of host cysteine proteases by the fungal effector Pit2. PLoS Pathog. 2013;9(2):e1003177. doi: 10.1371/journal.ppat.1003177. PubMed PMID: 23459172; PubMed Central PMCID: PMC3573112.

833 58. Misas Villamil JC, Mueller AN, Demir F, Meyer U, Ökmen B, Schulze Hüynck J, et al.
834 A fungal substrate mimicking molecule suppresses plant immunity via an inter-kingdom
835 conserved motif. Nature communications. 2019;10(1):1576. Epub 2019/04/07. doi:
836 10.1038/s41467-019-09472-8. PubMed PMID: 30952847; PubMed Central PMCID:
837 PMCPMC6450895.
838 59. Plett JM, Kemppainen M, Kale SD, Kohler A, Legue V, Brun A, et al. A secreted
839 effector protein of *Laccaria bicolor* is required for symbiosis development. Curr Biol.
840 2011;21(14):1197-203. doi: 10.1016/j.cub.2011.05.033. PubMed PMID: 21757352.
841 60. Plett JM, Daguerre Y, Wittulsky S, Vayssieres A, Deveau A, Melton SJ, et al. Effector
842 MiSSP7 of the mutualistic fungus *Laccaria bicolor* stabilizes the Populus JAZ6 protein and
843 represses jasmonic acid (JA) responsive genes. Proc Natl Acad Sci USA. 2014;111(22):8299-
844 304. doi: 10.1073/pnas.1322671111. PubMed PMID: 24847068; PubMed Central PMCID:
845 PMC4050555.
846 61. Wessling R, Epple P, Altmann S, He Y, Yang L, Henz SR, et al. Convergent targeting of
847 a common host protein-network by pathogen effectors from three kingdoms of life. Cell Host
848 Microbe. 2014;16(3):364-75. Epub 2014/09/12. doi: 10.1016/j.chom.2014.08.004. PubMed
849 PMID: 25211078; PubMed Central PMCID: PMC4191710.
850 62. Win J, Chaparro-Garcia A, Belhaj K, Saunders DG, Yoshida K, Dong S, et al. Effector
851 biology of plant-associated organisms: concepts and perspectives. Cold Spring Harbor symposia
852 on quantitative biology. 2012;77:235-47. Epub 2012/12/12. doi: 10.1101/sqb.2012.77.015933.
853 PubMed PMID: 23223409.

854 63. Eaton CJ, Dupont P-Y, Solomon PS, Clayton W, Scott B, Cox MP. A core gene set
855 describes the molecular basis of mutualism and antagonism in *Epichloë* species. Mol Plant-
856 Microbe Interact. 2015;28:218-31. doi: doi.org/10.1094/MPMI-09-14-0293-FI.
857 64. Rouxel T, Grandaubert J, Hane JK, Hoede C, van de Wouw AP, Couloux A, et al.
858 Effector diversification within compartments of the *Leptosphaeria maculans* genome affected by
859 Repeat-Induced Point mutations. Nature communications. 2011;2:202. doi:
860 10.1038/ncomms1189. PubMed PMID: 21326234; PubMed Central PMCID: PMC3105345.
861 65. Lo Presti L, Lanver D, Schweizer G, Tanaka S, Liang L, Tollot M, et al. Fungal effectors
862 and plant susceptibility. Annu Rev Plant Biol. 2015;66:513-45. doi: 10.1146/annurev-arplant-
863 043014-114623. PubMed PMID: 25923844.
864 66. Becker M, Becker Y, Green K, Scott B. The endophytic symbiont *Epichloë festucae*
865 establishes an epiphyllous net on the surface of *Lolium perenne* leaves by development of an
866 expressorium, an appressorium-like leaf exit structure. New Phytol. 2016;211:240-54. doi:
867 10.1111/nph.13931. PubMed PMID: 26991322.
868 67. Soyer JL, El Ghalid M, Glaser N, Ollivier B, Linglin J, Grandaubert J, et al. Epigenetic
869 control of effector gene expression in the plant pathogenic fungus *Leptosphaeria maculans*.
870 PLoS Genet. 2013;10(3):e1004227. Epub 2014/03/08. doi: 10.1371/journal.pgen.1004227
871 PGENETICS-D-13-03255 [pii]. PubMed PMID: 24603691; PubMed Central PMCID:
872 PMC3945186.
873 68. Itoh Y, Johnson R, Scott B. Integrative transformation of the mycotoxin-producing
874 fungus, *Penicillium paxilli*. Curr Genet. 1994;25:508-13.

875 69. Young CA, Bryant MK, Christensen MJ, Tapper BA, Bryan GT, Scott B. Molecular
876 cloning and genetic analysis of a symbiosis-expressed gene cluster for lolitrem biosynthesis from
877 a mutualistic endophyte of perennial ryegrass. Mol Gen Genomics. 2005;274:13-29.
878 70. Latch GCM, Christensen MJ. Artificial infection of grasses with endophytes. Ann Appl
879 Biol. 1985;107(1):17-24.
880 71. Tanaka A, Tapper BA, Popay A, Parker EJ, Scott B. A symbiosis expressed non-
881 ribosomal peptide synthetase from a mutualistic fungal endophyte of perennial ryegrass confers
882 protection to the symbiotum from insect herbivory. Mol Microbiol. 2005;57(4):1036-50.
883 72. Gibson DG, Young L, Chuang RY, Venter JC, Hutchison CA, III, Smith HO. Enzymatic
884 assembly of DNA molecules up to several hundred kilobases. Nature Methods. 2009;6(5):343-5.
885 Epub 2009/04/14. doi: nmeth.1318 [pii]
886 10.1038/nmeth.1318. PubMed PMID: 19363495.
887 73. Southern EM. Detection of specific sequences among DNA fragments separated by gel
888 electrophoresis. J Mol Biol. 1975;98:503-17.
889 74. Stone BA, Evans NA, Bonig I, Clarke AE. The application of sirofluor, a chemically
890 defined fluorochrome from aniline blue for the histochemical detection of callose. Protoplasma.
891 1984;122:191-5.
892 75. Letunic I, Doerks T, Bork P. SMART: recent updates, new developments and status in
893 2015. Nucleic Acids Res. 2015;43(Database issue):D257-60. Epub 2014/10/11. doi:
894 10.1093/nar/gku949. PubMed PMID: 25300481; PubMed Central PMCID: PMC4384020.
895 76. Schultz J, Milpetz F, Bork P, Ponting CP. SMART, a simple modular architecture
896 research tool: identification of signaling domains. Proc Natl Acad Sci USA. 1998;95(11):5857-

64. Epub 1998/05/30. doi: 10.1073/pnas.95.11.5857. PubMed PMID: 9600884; PubMed Central PMCID: PMCPMC34487.

77. Goujon M, McWilliam H, Li W, Valentin F, Squizzato S, Paern J, et al. A new bioinformatics analysis tools framework at EMBL-EBI. Nucleic Acids Res. 2010;38(Web Server issue):W695-9. Epub 2010/05/05. doi: 10.1093/nar/gkq313. PubMed PMID: 20439314; PubMed Central PMCID: PMCPMC2896090.

78. Sievers F, Wilm A, Dineen D, Gibson TJ, Karplus K, Li W, et al. Fast, scalable generation of high-quality protein multiple sequence alignments using Clustal Omega. Mol Syst Biol. 2011;7:539. Epub 2011/10/13. doi: 10.1038/msb.2011.75. PubMed PMID: 21988835; PubMed Central PMCID: PMCPMC3261699.

79. Andrews S. FastQC: a quality control tool for high throughput sequence data. Available online at: http://www.bioinformatics.babraham.ac.uk/projects/fastqc2010.

80. Bolger AM, Lohse M, Usadel B. Trimmomatic: a flexible trimmer for Illumina sequence data. Bioinformatics. 2014;30(15):2114-20. Epub 2014/04/04. doi: 10.1093/bioinformatics/btu170. PubMed PMID: 24695404; PubMed Central PMCID: PMCPMC4103590.

81. Patro R, Duggal G, Love MI, Irizarry RA, Kingsford C. Salmon provides fast and bias-aware quantification of transcript expression. Nat Methods. 2017;14(4):417-9. Epub 2017/03/07. doi: 10.1038/nmeth.4197. PubMed PMID: 28263959; PubMed Central PMCID: PMCPMC5600148.

82. R development core team. R: A language and environment for statistical computing. R Foundation for Statistical Computing, Vienna, Austria. 2020;URL https://www.R-project.org/.

919 83. Soneson C, Love MI, Robinson MD. Differential analyses for RNA-seq: transcript-level
920 estimates improve gene-level inferences. F1000Res. 2015;4:1521. Epub 2016/03/01. doi:
921 10.12688/f1000research.7563.2. PubMed PMID: 26925227; PubMed Central PMCID:
922 PMCPMC4712774.
923 84. Love MI, Huber W, Anders S. Moderated estimation of fold change and dispersion for
924 RNA-seq data with DESeq2. Genome Biol. 2014;15(12):550. Epub 2014/12/18. doi:
925 10.1186/s13059-014-0550-8. PubMed PMID: 25516281; PubMed Central PMCID:
926 PMCPMC4302049.
927 85. Zhu A, Ibrahim JG, Love MI. Heavy-tailed prior distributions for sequence count data:
928 removing the noise and preserving large differences. Bioinformatics. 2019;35(12):2084-92. Epub
929 2018/11/06. doi: 10.1093/bioinformatics/bty895. PubMed PMID: 30395178; PubMed Central
930 PMCID: PMCPMC6581436.
931 86. Stephens M. False discovery rates: a new deal. Biostatistics. 2017;18(2):275-94. Epub
932 2016/10/21. doi: 10.1093/biostatistics/kxw041. PubMed PMID: 27756721; PubMed Central
933 PMCID: PMCPMC5379932.
934 87. Almagro Armenteros JJ, Tsirigos KD, Sønderby CK, Petersen TN, Winther O, Brunak S,
935 et al. SignalP 5.0 improves signal peptide predictions using deep neural networks. Nat
936 Biotechnol. 2019;37(4):420-3. Epub 2019/02/20. doi: 10.1038/s41587-019-0036-z. PubMed
937 PMID: 30778233.
938 88. Nielsen H, Engelbrecht J, Brunak S, von Heijne G. Identification of prokaryotic and
939 eukaryotic signal peptides and prediction of their cleavage sites. Protein Eng. 1997;10(1):1-6.
940 PubMed PMID: 9051728.

941 89. Törönen P, Medlar A, Holm L. PANNZER2: a rapid functional annotation web server.

942 Nucleic Acids Res. 2018;46(W1):W84-W8. Epub 2018/05/10. doi: 10.1093/nar/gky350.

943 PubMed PMID: 29741643; PubMed Central PMCID: PMCPMC6031051.

944

945

946

947 **Table 1.** Host infection rates of *setB* and *clrD* mutants.

	Wild-type	**Δ*setB***	**Δ*setB*/*setB***	**Δ*setB*/*setB*$^{(C254A)}$**
Expt 1	20/37 (54%)	0/44 (0%)	18/27 (67%)	10/38 (26%)
Expt 2	28/32 (88%)	0/35 (0%)	33/54 (61%)	8/85 (9%)
Expt 3	33/46 (72%)	0/36 (0%)		
Expt 4	21/28 (75%)	0/41 (0%)		
	Wild-type	**Δ*clrD*/*clrD***	**Δ*clrD*/*clrD*$^{(C265A)}$**	
Expt 1	10/15 (67%)	12/13 (92%)	0/52 (0%)	

948 Number of plants infected with the indicated strains, over the total number of plants in each
949 independent study. Percentages of infection are indicated in parentheses. Plants were analysed at
950 8-12 wpi.

951

952

953

954

955

956

Supporting Information

S1 Fig. Strategy for deletion of *E. festucae setB* and confirmation by Southern hybridisation analysis and PCR.

S2 Fig. Phenotype of plants infected with Δ*setB*/*setB*$^{(C254A)}$ strain. Plants were photographed at 8 wpi.

S3 Fig. Expression of host defense genes in *ΔsetB*- and *ΔclrD*- inoculated plants.

S4 Fig. Co-inoculation with the wild-type strain allowed host infection by Δ*setB* and Δ*clrD*.

S5 Fig. Hyphal fusion ability is not affected in Δ*setB* and *ΔclrD*.

S6 Fig. Immunoblot and phenotype of co-inoculated plants at 8 wpi .

S7 Fig. Host stunting correlates with the presence of mutant hyphae in co-inoculated plants.

S8 Fig. Candidate infection genes are located near AT-rich or repeat-rich regions.

S9 Fig. Chromosome location of four candidate infection genes in *E. festucae* strain Fl1.

S10 Fig. Microsyntenic comparison of the 10 kb *crbA* loci in *Epichloë* species possessing *crbA* orthologs.

S11 Fig. Strategy for deletion of *E. festucae crbA*, *dmlA*, *hybC* and overexpression of *sspZ*.

S12 Fig. Culture phenotype of *E. festucae* wild-type, *crbA*, *dmlA*, *hybC* and *sspZ* mutants on PDA.

S13 Fig. Plant infection phenotype for *E. festucae crbA*, *dmlA*, *hybC* and *sspZ* mutants.

977 **File S1. Differences in gene expression between *E. festucae* WT and either Δ*clrD* or Δs*etB* at**
978 **3 dpi in *L. perenne*.**

979 **File S2. Differences in gene expression between *E. festucae* WT in planta at 3 dpi versus in**
980 **axenic culture.**

981 **File S3. Differences in gene expression of *L. perenne* infected with *E. festucae* WT and mock**
982 **infected.**

983 **File S4. Differences in gene expression of *L. perenne* infected with *E. festucae* WT and either**
984 **Δ*clrD* or Δs*etB* at 3 dpi.**

985 **Table S1: Homologues of *crbA* and *dmlA* in other *Epichloe* species.**

986 **Table S2: Host infection rates of *E. festucae crbA*, *dmlA*, *hybC* and *sspZ* mutants.**

987 **Table S3: Biological material.**

988 **Table S4: Primers used in this study.**

989 **Table S5: Biosample numbers for transcriptome data.**

990

991

992

993

994

Author Contributions

Conceptualization: Yonathan Lukito, Tetsuya Chuo, David J. Winter, Murray P. Cox, Barry Scott.

Data curation: Kate Lee, David J. Winter.

Formal analysis: Yonathan Lukito, Kate Lee, Nazanin Noorifar, Kimberly A. Green, David J. Winter, Tracy K. Hale, Tetsuya Chuo, Linda J. Johnson, Murray P. Cox, Barry Scott

Funding acquisition: Linda J. Johnson, Murray P. Cox, Barry Scott

Investigation: Yonathan Lukito, Kate Lee, Nazanin Noorifar, Kimberly A. Green, David J. Winter, Arvina Ram,

Project administration: Tracy K. Hale, Tetsuya Chuo, Linda J. Johnson, Murray P. Cox, Barry Scott

Resources: Linda J. Johnson, Murray P. Cox, Barry Scott

Software: Kate Lee, David J. Winter, Murray P. Cox,

Supervision: Tracy K. Hale, Tetsuya Chuo, Linda J. Johnson, Murray P. Cox, Barry Scott

Writing: Yonathan Lukito, Barry Scott